Deep-Sea Research I 56 (2009) 909–925

Contents lists available at ScienceDirect

Deep-Sea Research I

journal homepage: www.elsevier.com/locate/dsri

# On the role of mesoscale eddies in the ventilation of Antarctic intermediate water

Zouhair Lachkar [a,*], James C. Orr [b], Jean-Claude Dutay [c], Pascale Delecluse [d]

[a] Environmental Physics, Institute of Biogeochemistry and Pollutant Dynamics, ETH Zurich, Universitätstrasse 16, 8092 Zurich, Switzerland
[b] Marine Environment Laboratories, International Atomic Energy Agency, 4 Quai Antoine Premier, MC98000 Monaco, Monaco
[c] LSCE-IPSL, Laboratoire des Sciences du Climat et de l'Environnement CEA Saclay, L'Orme des Merisiers, Gif-sur-Yvette 91911, France
[d] Meteo-France, Centre National de Recherches Météorologiques, 2 avenue Rapp, 75340 Paris, France

ARTICLE INFO

*Article history:*
Received 29 June 2008
Received in revised form
5 January 2009
Accepted 15 January 2009
Available online 5 February 2009

*Keywords:*
AAIW
Mesoscale eddies
CFC-11
Ventilation
Southern Ocean

ABSTRACT

The spatial distribution of Antarctic intermediate water (AAIW) formation and ventilation remains a matter of debate. Some studies suggest that AAIW forms nearly homogeneously in a circumpolar pattern, whereas others favor more localized formation particularly in the southeast Pacific Ocean. We show here that the patterns and magnitude of AAIW formation and ventilation are substantially affected by mesoscale eddies. To diagnose the role of eddies, we made global CFC-11 simulations in two versions of the ocean general circulation model OPA9, a "non-eddying", coarse-resolution version ($2^\circ \cos\varphi \times 2^\circ$, ORCA2) and an "eddying" or eddy-permitting version ($\frac{1}{2}^\circ \cos\varphi \times \frac{1}{2}^\circ$, ORCA05). In the non-eddying simulation, AAIW subducts in a near homogeneous, circumpolar pattern; in the eddying simulation, the distribution of AAIW ventilation is patchier. Increasing resolution causes the AAIW layer to thin by 32% on average in the Indian sector, but only by 11% in the Pacific sector. This patchiness appears due to the zonal wind stress, which is weak over much of the Pacific and southwest Atlantic sectors but is strong over the Indian sector. Consequently, the effect of eddies is largest in the Indian Ocean, moderate in the Atlantic, and smallest in the Pacific basin. Although the Gent and McWilliams (GM) eddy parameterization improves the overall vertical structure of density in the Southern Ocean, applying it in our non-eddying model still results in the nearly uniform circumpolar distribution of AAIW ventilation, in contrast to the observations.



## 1. Introduction

The Antarctic intermediate water (AAIW) can be identified as a tongue of freshwater at intermediate depths (McCartney, 1977, 1982; Rintoul et al., 2001) observed in all sectors of the Southern Hemisphere oceans north of the subantarctic front (SAF), which defines the northern boundary of the Antarctic circumpolar current (ACC). As a key component of the upper branch of the global thermohaline circulation (Schmitz, 1996), AAIW plays a crucial role in closing the hydrological cycle by providing the ocean route by which freshwater from excess precipitation in the high latitudes is returned to the tropics. Furthermore, the AAIW helps to sequester most of the anthropogenic tracers taken up from the atmosphere by the Southern Ocean (Fine, 1993; Fine et al., 2001; Sabine et al., 2002, 2004). The southern extratropics are also where one finds the largest uncertainties in model estimates of ocean storage of anthropogenic $CO_2$ and CFC-11, particularly at intermediate depths (Orr et al., 2001; Dutay et al., 2002). Hence an improved understanding of the formation and ventilation of AAIW is

* Corresponding author. Tel.: +41 44 632 08 94; fax: +41 44 632 16 91.
*E-mail address:* zouhair.lachkar@env.ethz.ch (Z. Lachkar).

0967-0637/$ - see front matter © 2009 Elsevier Ltd. All rights reserved.
doi:10.1016/j.dsr.2009.01.013

needed to refine estimates of ocean uptake of anthropogenic $CO_2$, which also affects the magnitude of future climate change (Sarmiento and Le Quéré, 1996; Sabine and Feely, 2001; Sabine et al., 2004).

The processes that control the AAIW formation have fueled a long debate about the location of its source regions. Sverdrup et al. (1942) suggested that AAIW results from isopycnal subduction of Antarctic surface water (AASW) that occurs homogeneously along the ACC. In contrast, McCartney (1977) argued that AAIW is essentially formed by the deep convection in the extreme eastern South Pacific Ocean from the densest classes of subantarctic mode water (SAMW). Observational studies have supported either the circumpolar view (Molinelli, 1981; Piola and Georgi, 1982) or the localized hypotheses (Talley, 1996; Rintoul et al., 2001) of AAIW formation. Similar disagreement occurs in simulations using coarse-resolution ocean general circulation models (OGCMs). Models by Marsh et al. (2000) and Sorensen et al. (2001) simulate AAIW forming homogeneously along the SAF via direct subduction from the surface towards the interior. Conversely, simulations by England et al. (1993) and Saenko and England (2003) support the localized view of McCartney (1977). Why then do models differ?

Part of the answer, as we shall show here, lies in how eddies are represented in these models. Several previous studies have suggested that mesoscale eddies do affect the key processes involved in the formation and subduction of AAIW. For example, Marshall (1997) used an idealized 2-D ocean model and found that mesoscale eddies modify the rate of watermass transfer from the surface mixed layer into the interior thermocline in regions of intense baroclinic instability such as the ACC. Lee et al. (1997) showed that eddy-induced advection is a key control of decadal-scale, meridional transfer across a zonal jet (e.g., for northward advection of dense AASW across the SAF). This meridional transfer of AASW feeds the AAIW both directly by isopycnal subduction and indirectly through the surface SAMW layer (Ribbe, 1999).

Parameterized eddies have also been shown to substantially impact the circulation and the structure of the flow at the latitudes of AAIW subduction. For instance, in most coarse-resolution OGCM simulations that use the Gent and McWilliams (GM) approach to parameterize effects of mesoscale eddies (Gent and McWilliams, 1990; Gent et al., 1995), isopycnal subduction of dense surface water dominates AAIW formation (Danabasoglu et al., 1994; Hirst and Cai, 1994; Sorensen et al., 2001). The GM parameterization increases vertical stratification and reduces the wintertime convection (Hirst and McDougall, 1996; England and Hirst, 1997). The importance of mesoscale eddies in setting the vertical stratification was also demonstrated in several theoretical studies (Vallis, 2000; Marshall and Radko, 2003).

Despite these advances, there remains a poor understanding of how mesoscale eddies affect AAIW subduction and ventilation. Furthermore, the most widely used GM scheme is an adiabatic eddy parameterization. Thus it misrepresents near-surface eddy fluxes, which have an important diabatic component (Price, 2001; Ferrari et al., 2008; Ferreira and Marshall, 2006). The GM scheme's misrepresentation of the eddy diapycnal flux in the mixed layer could drive spurious exchange between the upper mixed layer and ocean interior, thereby impacting simulated intermediate water ventilation and formation.

Here we explore how the thickness and the patterns of simulated AAIW change as one crosses the threshold where a model begins to explicitly resolve mesoscale eddies, i.e., when moving from a coarse-resolution to an eddy-permitting OGCM allowing for a highly nonlinear and non-diffusive dynamics to develop. To isolate the effect of eddies, we compare integrations of a coarse-resolution and a relatively high-resolution versions of the ORCA model, neither of which incorporate a GM parameterization, as detailed by Lachkar et al. (2007). Additionally, by comparing the eddy-permitting model to a second simulation of the coarse-resolution model, but this time with GM, we evaluate the ability of GM to mimic how explicitly resolved eddies affect simulated AAIW ventilation in the southern extratropics.

To evaluate intermediate water ventilation, we included CFC-11 as a passive tracer in all versions of the model. Others have used CFC-11 to evaluate ocean decadal timescale ventilation and general model performance (England, 1995; Dixon et al., 1996; Doney et al., 1998; Dutay et al., 2002; Sasai et al., 2004; Sen Gupta and England, 2004). The spatial distribution and the temporal evolution of CFC-11 concentrations within the AAIW layer help locate where there is enhanced AAIW ventilation and subduction.

## 2. Methods

Our simulations of the general ocean circulation were made with the ORCA-LIM global ice-ocean model, or more precisely the ocean model OPA (Océan PArallélisé, version 9) coupled to the dynamic-thermodynamic Louvain-la-Neuve sea-ice model (LIM) (Fichefet and Maqueda, 1997). A full description of OPA is provided in Madec and Imbard (1996) and Madec et al. (1998). The model has 46 vertical levels with a vertical grid resolution varying from 6 m at the surface to 250 m at the bottom. Vertical mixing coefficients are computed from a second-order closure scheme based on a prognostic equation for turbulent kinetic energy (TKE) (Gaspar et al., 1990; Blanke and Delecluse, 1997). Lateral tracer mixing occurs along isopycnal surfaces (Cox, 1987). Further details of the model physics are given in Lachkar et al. (2007).

The bathymetry is calculated using the 2′ bathymetry file ETOPO2 from NGDC (National Geophysical Data Center) (Smith and Sandwell, 1997; Jakobsson et al., 2000), except for the zone south of 72°S where it was computed from the BEDMAP data (Lythe and Vaughan, 2001). Initial conditions for the temperature and salinity fields were taken from Levitus et al. (1998) for the low and middle latitudes and from the PHC2.1 climatology (Steele et al., 2001) for high latitudes. The model was started from rest, then spun up for 8 years with a climatological seasonal forcing with daily frequency as computed from the 1992–2000 NCEP/NCAR 10-m wind stress and 2-m air temperature data (Kalnay et al., 1996).

Additionally, we used monthly climatologies of precipitation (Xie and Arkin, 1996), relative humidity (Trenberth et al., 1989), and total cloud cover (Berliand and Strokina, 1980). Surface heat fluxes and freshwater flux for ocean and sea-ice were calculated using the empirical bulk parametrization proposed by Goose (1997), which yields more realistic results than traditional restoring of sea-surface temperature and salinity (Large et al., 1997; Gent et al., 1998).

The non-eddying version of the ORCA model has a $2^\circ \cos\varphi \times 2^\circ$ ($\varphi$ is latitude) grid, whereas the eddying version of the same model has a $\frac{1}{2}^\circ \cos\varphi \times \frac{1}{2}^\circ$ grid. In the eddying simulation, the average grid size is 34 km (27 km at 60°S). Although the eddying model leaves an important part of the mesoscale eddy spectrum unresolved, it does allow substantial mesoscale eddy activity to develop in the Southern Ocean and near western boundary currents (Fig. 1). A third simulation was conducted in the non-eddying version of the model where the GM parameterization was included. The coefficient of isopycnal diffusivity in this simulation was set to $2 \times 10^3\,\mathrm{m^2\,s^{-1}}$. The GM thickness diffusivity $k_{eddy}$ varies with the first baroclinic Rossby radius $L_R = NH/f$ and the baroclinic growth rate $\sigma^{-1} = f/\sqrt{Ri}$ following the Visbeck et al. (1997) formulation:

$$k_{eddy} = \alpha\sigma^{-1}L_R^2 \tag{1}$$

where $H$ is the ocean depth, $f$ is the Coriolis parameter, $\alpha = 0.016$ is a proportionality constant, $Ri = f^2 s_\rho^2 N^2$ is the Richardson number of large-scale flow, $s_\rho$ is the vertically averaged isopycnal slope, and $N^2$ is a representation of the mean stratification (Brunt–Väisälä frequency). To ensure that the eddy-induced transport vanishes at the boundaries, a linear tapering of the slope is applied from its ocean interior value just below the mixed layer to zero at the surface.

Results of these simulations were analyzed in an isopycnal coordinate framework in order to facilitate diagnosis of isopycnal subduction of water masses in the Southern Ocean and to better evaluate CFC-11 patterns within the AAIW layer. Thus, model output was projected onto 71 evenly spaced $\sigma_0$ potential density layers ranging from 21 to 28. The $\sigma_0 = 27.2$ isopycnal surface, which is often used to track AAIW (Sorensen et al., 2001; Karsten and Marshall, 2002; Santoso and England, 2004), lies within the core of this intermediate water in the three simulations. Here we use the range 27.0–27.4 to characterize AAIW class of water masses.

To reduce the computational cost, we made the CFC-11 simulations using an offline approach. The offline model was driven by 5-day snapshots of 3-D fields of advection and vertical turbulent diffusion simulated by the dynamic (online) model. The simulations for CFC-11 were made using the tracer-transport version of OPA (OPA Tracer 8.5), more details of which are provided by Lachkar et al. (2007). To model CFC-11 ocean uptake, we followed the OCMIP-2 protocols (Dutay et al., 2002). The CFC-11 (chlorofluorocarbon-11) is a purely anthropogenic passive tracer that was first introduced in the atmosphere in the 1930s (Gammon et al., 1982; Wallace and Lazier, 1988;

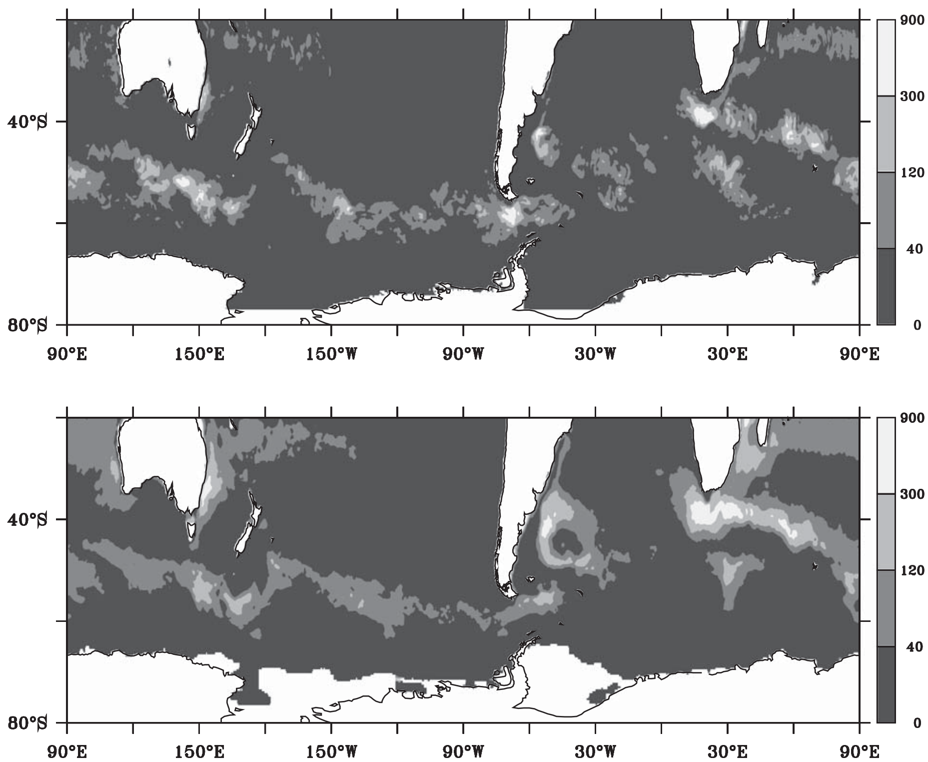


**Fig. 1.** Map of eddy kinetic energy (EKE) in the eddying model (top) and from TOPEX observations (bottom) in $\mathrm{cm^2\,s^{-2}}$ south of 20°S. The observed EKE is divided by a factor of 4 to better compare spatial patterns with the eddying model. The non-eddying's EKE is close to zero and not shown here.

Doney and Bullister, 1992). We initiated the offline simulations in 1950 because atmospheric CFC-11 concentrations before this date were less than 1% of the maximum in 1994. We evaluated simulated CFC-11 distributions by comparing them to the gridded data-based product from Global Ocean Data Analysis Project (GLODAP) (Key et al., 2004). The GLODAP product is based on a compilation of data from the World Ocean Circulation Experiment (WOCE), the Joint Global Ocean Flux Study (JGOFS), and the Ocean-Atmosphere Carbon Exchange Study (OACES).

## 3. Results

### 3.1. Structure of AAIW in the southern extratropics

The zonally averaged vertical density structure in the upper 3000 m between 70°S and 40°S (Fig. 2) reveals how explicitly accounting for eddies flattens isopycnal surfaces, lessening the abrupt increase in isopycnal layer thicknesses that characterizes the ACC frontal system in coarse-resolution models. This flattening primarily occurs below 100 m through to intermediate depths to the south of 40°S. This figure also shows a remarkable overall similarity between the eddying model and the non-eddying model with GM. Yet, it is well known that the path of the ACC undergoes important meridional displacements in regions of strong topography. Therefore, zonal averaging can lead to an unrealistic view of the overturning circulation across the meandering jet (Ivchenko et al., 1996). That is, the permanent meanders, also called "standing eddies", do substantially contribute to the meridional volume transport (Hallberg and Gnanadesikan, 2001; Lee and Coward, 2003). Thus, the differences in the zonal averaged density structure may not be fully due to the action of transient eddies. In order to clearly identify the relative importance of the transient eddies in setting the stratification and the density structure across the ACC we used a streamwise-average approach. By definition, the effects of standing eddies vanish when averaging is along streamlines (Marshall et al., 1993; Hallberg and Gnanadesikan, 2001; Karsten and Marshall, 2002). Using either barotropic or geostrophic streamfunctions gave similar results. Fig. 3 shows potential density averaged along barotropic streamlines in the three simulations. To capture the truly circumpolar flow, we calculated the streamwise average of density for the region bounded by the northernmost and southernmost lines of constant barotropic transport that pass through the Drake Passage (Fig. 3).

Although the contrast between the eddying and non-eddying models is reduced when averaging along streamlines, isopycnal surfaces are still much flatter in the higher resolution simulation. This flattening is due to the tendency of the transient eddies to weaken the baroclinicity of the mean flow by reducing its available potential energy (APE) (Gille et al., 1987; Pedlosky, 1987). Thus the

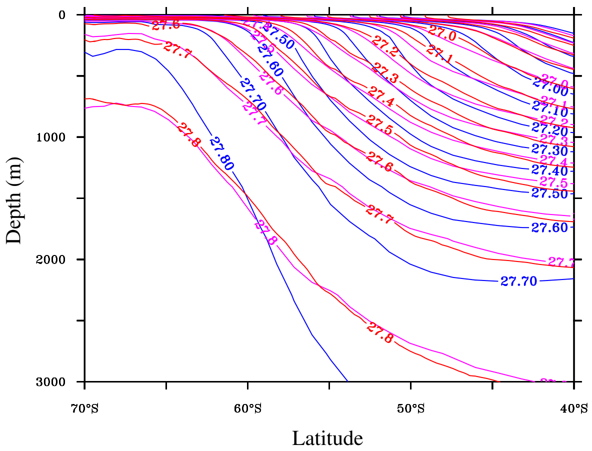


**Fig. 2.** Zonally averaged, annual mean, potential density south of 40°S for the upper 3000 m as simulated by the non-eddying model (blue), the eddying model (red) and the non-eddying model with GM (purple). South of 60°S, isopycnals near the surface are more diffuse in the eddying simulation, largely because of the thickening of the UCDW. (For interpretation of the references to color in this figure legend, the reader is referred to the web version of this article.)

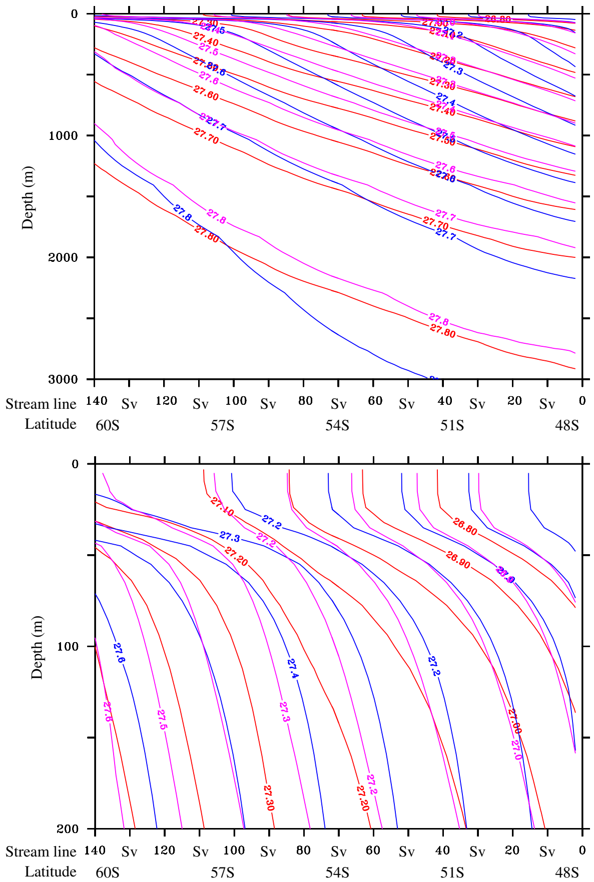


**Fig. 3.** Potential density averaged along bartropic streamlines for the upper 3000 m (top) and for only the upper 200 m (bottom), as simulated by the non-eddying model (blue), the eddying model (red) and the non-eddying model with GM (purple). The northernmost and southernmost bounds of the barotropic transport that go through the Drake Passage are 0 and 140 Sv, respectively. For clarity, the mean latitudes of streamlines are also indicated on the meridional coordinate axis. (For interpretation of the references to color in this figure legend, the reader is referred to the web version of this article.)

eddying simulation has denser water masses at intermediate depths and in the lower thermocline north of the polar front (PF) (60°S) and water masses with lower densities in the upper thermocline further south. These findings are consistent with previous studies showing that models that explicitly account for eddies also exhibit greater vertical stratification in the Southern Ocean (Vallis, 2000; Marshall et al., 2002; Marshall and Radko, 2003). Relative to the eddying model, the non-eddying model with GM shows a small systematic bias towards slightly denser waters at all depths when averaging along streamlines. These discrepancies are largest near ocean surface (Fig. 3). Nevertheless, in the ocean interior the density structure (defined by the slope of isopycnal surfaces) in the non-eddying model with GM generally agrees with that in the eddying model. Such is expected given that GM is known to dramatically improve the density profile in coarse-resolution models (Danabasoglu et al., 1994; Duffy et al., 1997).

Besides the eddying model flattening of isopycnals, it also exhibits a general thinning of the AAIW layer, defined as the distance between the 27.0 and 27.4 isopycnals (Fig. 4). This thinning is unevenly distributed around the SAF. Thinning is greatest in the Indian Ocean and is also notable in the Atlantic basin and in the eastern portion of the Pacific Ocean (between 80°W and 130°W). Conversely, in the central and southwest Pacific, the AAIW layer thickness changes little although it extends a few degrees farther south. To better understand those differences between the eddying and the non-eddying simulations, we used CFC-11 to help discern intermediate water ventilation and AAIW subduction.

### 3.2. CFC-11 and ventilation of AAIW

Fig. 5 shows snapshots of the CFC-11 vertical inventories integrated over the AAIW layer from the eddying and the non-eddying simulations. Because the concentration of CFC-11 in the atmosphere rose rapidly, particularly during the 1950s, there was a rapid rate of increase in the air-sea CFC-11 flux over the Southern Ocean during this period. As a consequence, during the 1950s then, the CFC-11 inventory in the AAIW layer is mainly due to new local ventilation of water masses. From the 1960s onwards, zonal transport of older subducted AAIW plays an increasing role, homogenizing the circumpolar distribution. Thus, the CFC-11 vertical inventory in the AAIW layer in 1955 offers a better indicator of the spatial distribution of intermediate water subduction than do inventories from later years. In the non-eddying simulation, AAIW ventilation occurs in a near circumpolar band along the ACC, with enhanced subduction in the southeast Pacific Ocean and south of Australia. In contrast, in the eddying simulation, AAIW ventilation is concentrated in the Pacific and in the westernmost Atlantic sectors, but is nearly absent from the Indian and southeast Atlantic sectors. The spatial distribution of AAIW subduction in the eddying simulation fits better with the localized description of McCartney (1977).

We further explored differences in the ventilation of intermediate waters between the eddying and the non-eddying simulations by comparing CFC-11 along two meridional sections in the Indian and Pacific sectors of the southern extratropics (Fig. 6). Both models exhibit a sharper meridional density gradient and PF frontal

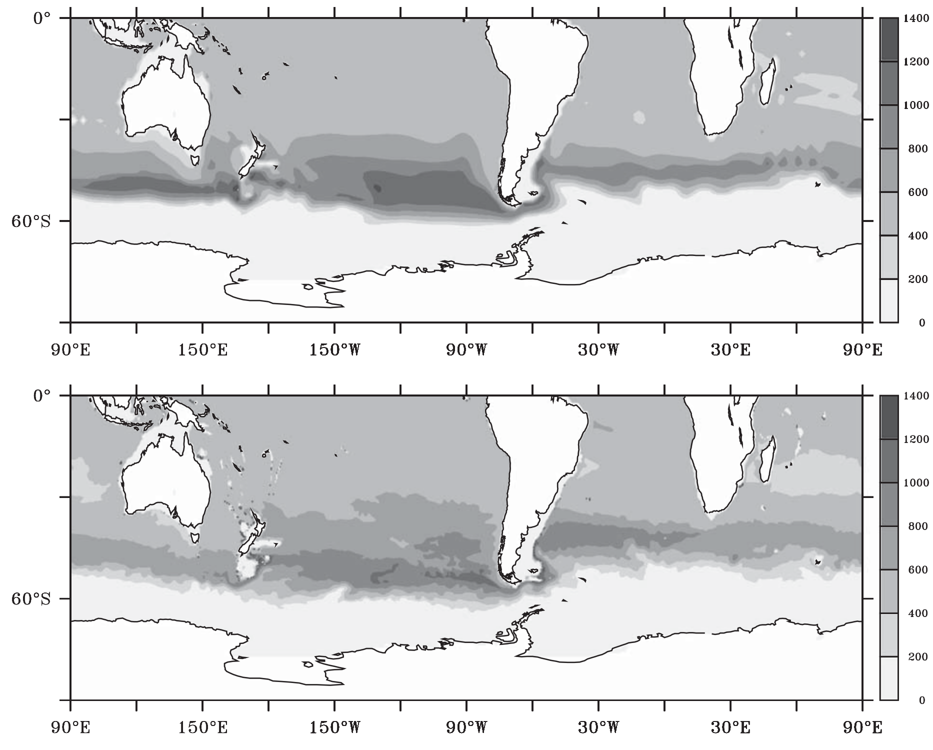


**Fig. 4.** Annual average AAIW layer thickness (m) from the non-eddying model (top) and the eddying model (bottom).

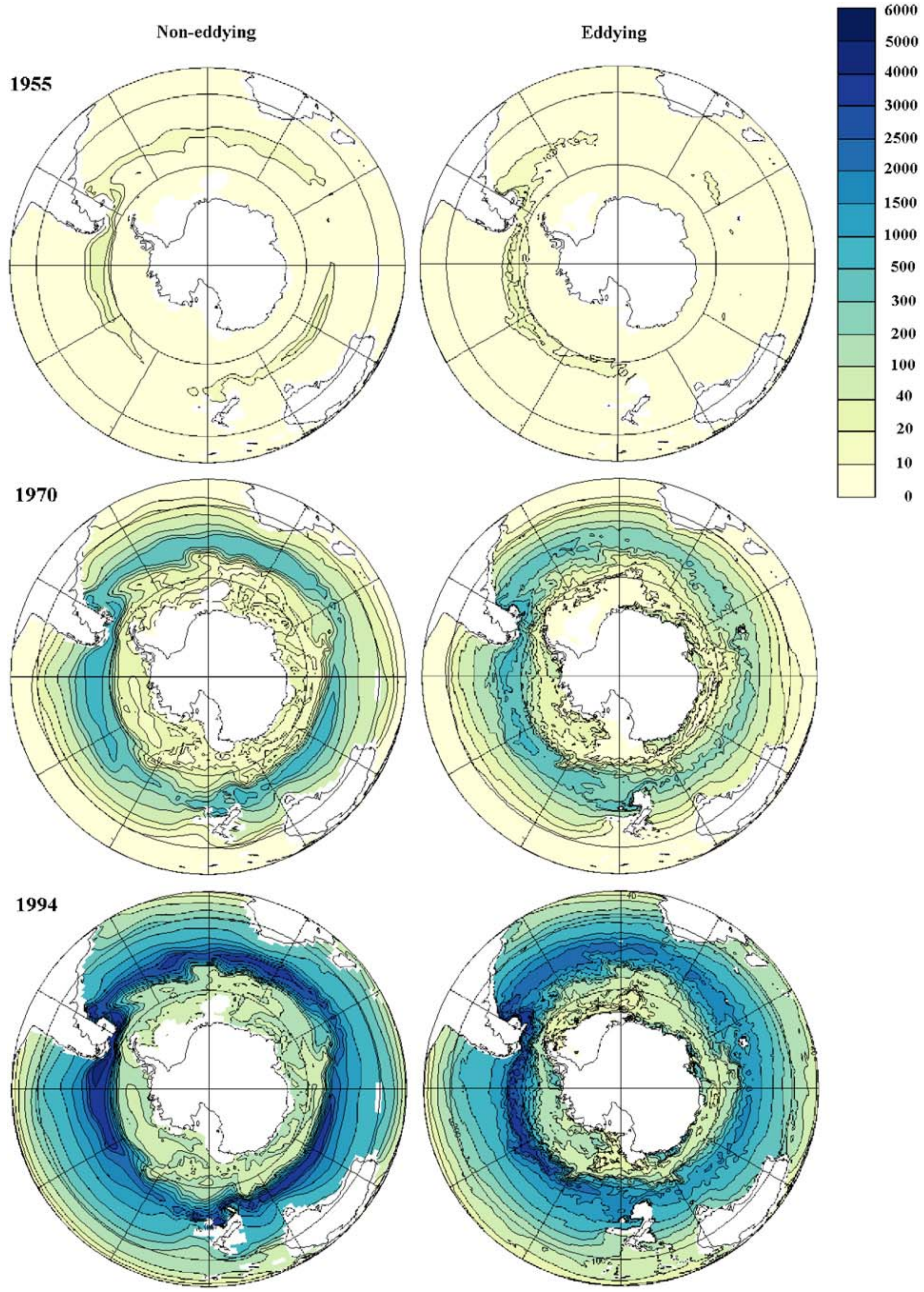


**Fig. 5.** Snapshots of CFC-11 inventory in the AAIW layer from the non-eddying model (left) and the eddying model (right) in 1955 (top), 1970 (middle), and 1994 (bottom). Inventories are given in pmol $m^{-2}$.

structure along the Indian section (along 125°E) relative to the Pacific section (along 90°W). In the Indian Ocean, there is only shallow CFC-11 penetration south of 60°S but a sharp gradient across the PF leads to much deeper penetration a few degrees to the north, particularly in the non-eddying simulation. Across both sections, the density field shows similar structure in the non-eddying model with GM relative to the eddying model. Yet, the CFC-11 penetrates substantially deeper in the non-eddying model with GM, indicating more rapid ventilation of the intermediate ocean in this model. For both sections, CFC-11 penetrates further across isopycnal surfaces in the non-eddying simulations both with and without GM. This suggests that the ventilation of intermediate water in the coarse-resolution simulations is not fully dominated by isopycnal subduction of surface water masses; additionally, diapycnal mixing and wintertime convection must be important for AAIW ventilation in these models. In contrast, the eddying simulation's greater tendency for CFC-11 contours to follow isopycnals, particularly in the

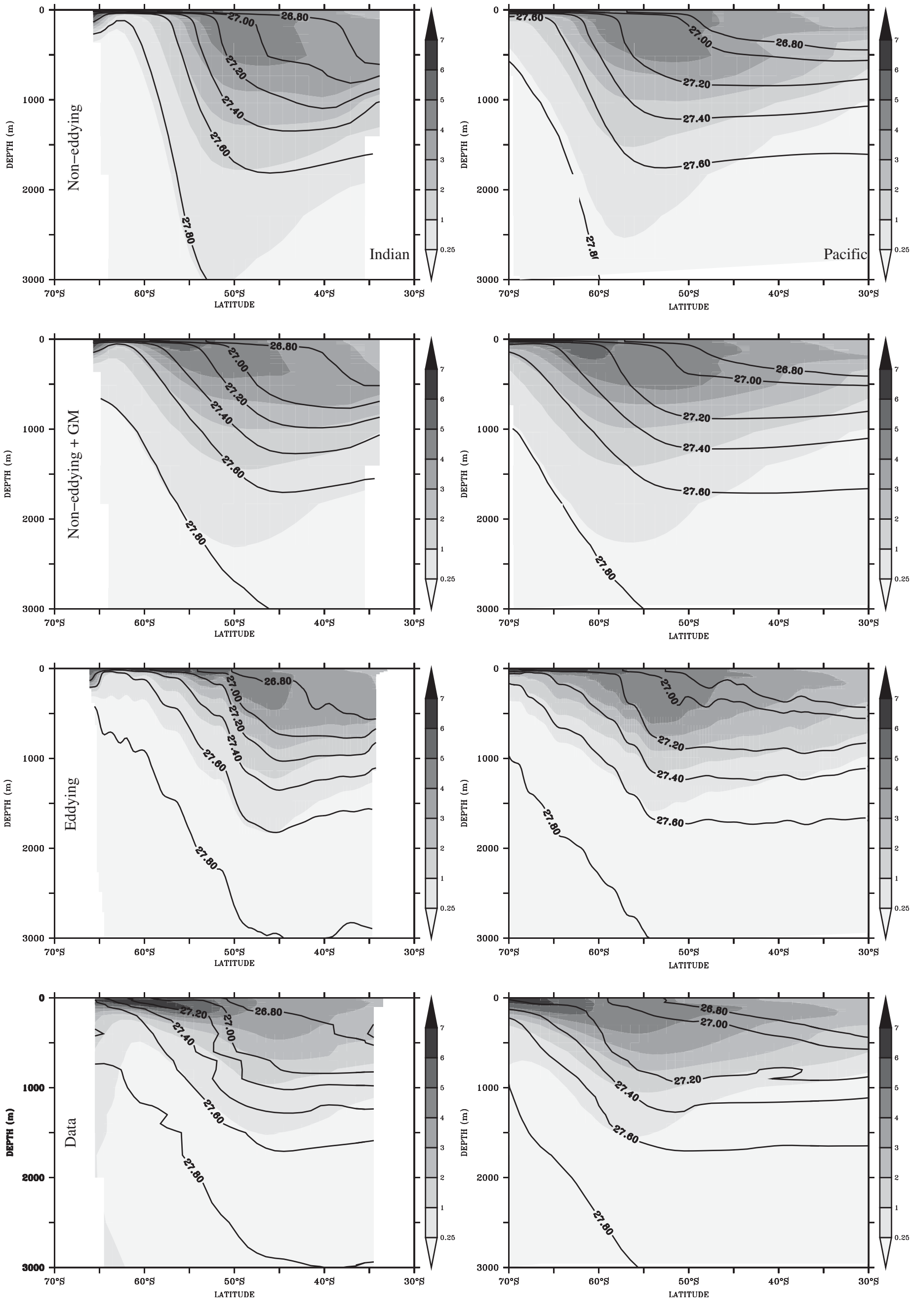


**Fig. 6.** The potential density field (black contours) superimposed over the CFC-11 concentration (in pmol $l^{-1}$) field (shading) along 125°E in the Indian Ocean (left) and 90°W in the Pacific Ocean (right) in 1994, as simulated by the non-eddying model (top row), the non-eddying model with GM (second row), the eddying model (third row) and from data (bottom row).

Indian Ocean (Fig. 6), suggests that explicitly resolving eddies allows isopycnal subduction to become the predominant mechanism by which AAIW is ventilated.

### 3.3. Comparison with observations

Fig. 6 also compares simulated CFC-11 concentrations to observations in 1994 along the same two sections. In the non-eddying simulation, the CFC-11 vertical distribution is too diffusive; it substantially overestimates the observed penetration, particularly in the Indian Ocean. The non-eddying model with GM shows a small improvement, illustrating that this parameterization slightly reduces the excessive ventilation of intermediate ocean. Still, CFC-11 vertical penetration is excessive in the non-eddying model with GM. There is greater general improvement due to the increase of horizontal resolution apparent in both sections, particularly the Indian section. Both sections exhibit more realistic vertical penetration of CFC-11 north of the SAF. South of 60°S, all models substantially underestimate tracer penetration. This artifact is due to a known deficiency of the ORCA model, which underestimates the mixed layer depth in highest southern latitudes (de Boyer Montégut et al., 2004; Lachkar et al., 2007). It appears to stem partly from vertical mixing in the mixed layer in this region being too weak in the current version of the model's TKE parameterization.

To further assess the extent to which including mesoscale eddies improves simulated AAIW ventilation, we compared the simulated AAIW inventory of CFC-11 to that observed in 1994 (Fig. 7). Overall, applying the GM parameterization improves the agreement of the non-eddying model with observations, particularly in the Atlantic sector where the model's excess CFC-11 inventory is substantially reduced. Yet, the non-eddying model with GM considerably overestimates the observed CFC-11 concentrations in the Indian sector and particularly south of Australia. This results in a more circumpolar and uniformly distributed AAIW ventilation along the ACC, compared to more localized, Pacific-enhanced, ventilation found with the eddying model (Fig. 7). Out of the three simulations, the eddying model exhibits the most realistic

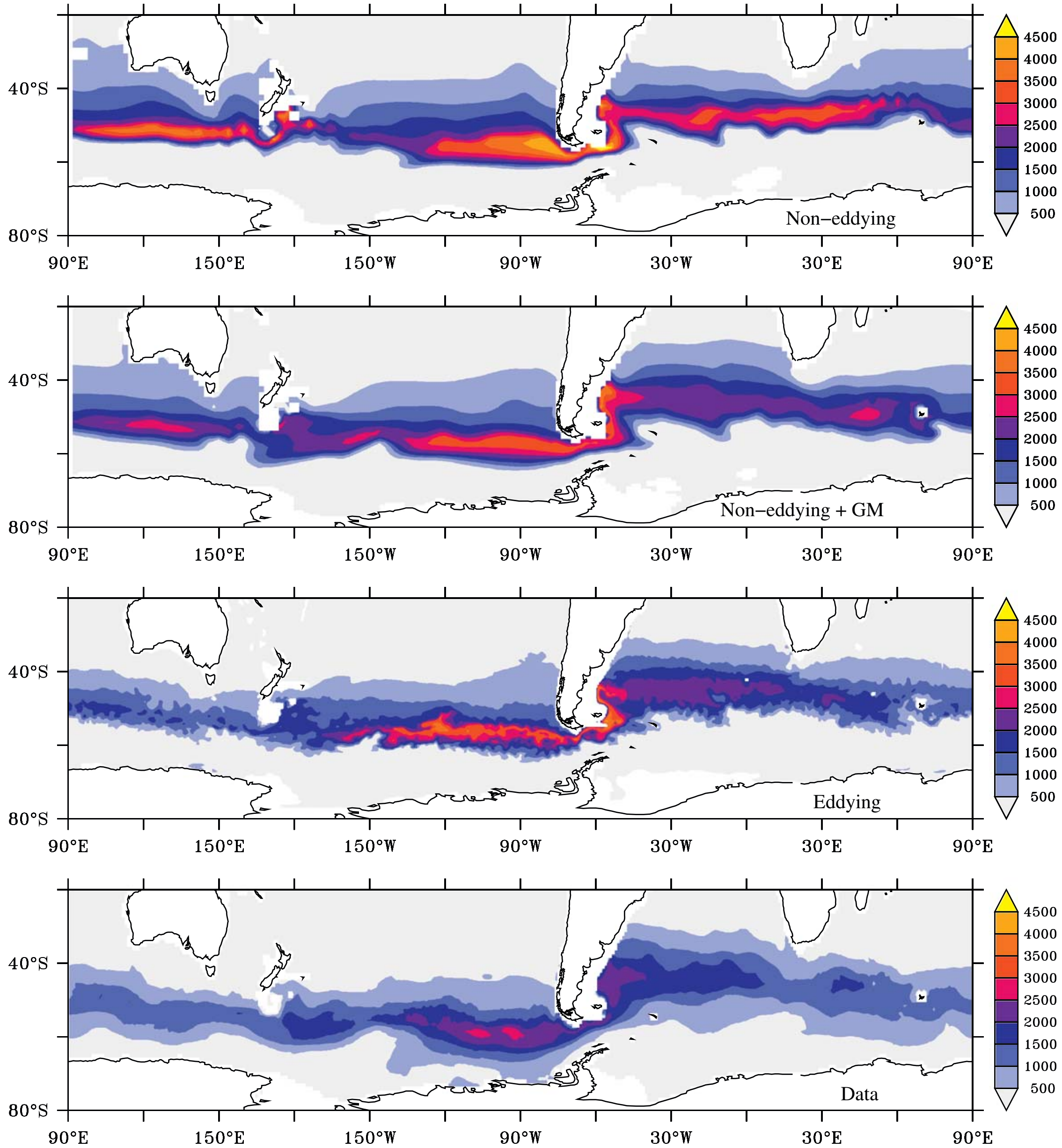


**Fig. 7.** The CFC-11 inventory in AAIW layer (pmol $m^{-2}$) in 1994 as (from top to bottom) simulated in the non-eddying model, the non-eddying model with the GM parameterization, the eddying model, and from the GLODAP data.

ventilation of AAIW, both in terms of the pattern and the overall magnitude of its CFC-11 inventory.

Overall, moving from the non-eddying model, with or without GM, to the eddying model improves the simulated AAIW subduction and ventilation of intermediate waters. The simulated CFC-11 inventory in the AAIW changes from having a nearly homogeneous circumpolar pattern to a more localized distribution centered about the southeast Pacific. Furthermore, by moving to the eddying model, isopycnal subduction of surface water masses appears to become the predominant means by which southern intermediate waters are ventilated, particularly in the Indian Ocean where the increase in resolution results in the largest decrease in AAIW formation. The mechanisms that are responsible for these changes are elucidated in the following section.

## 4. Discussion

### *4.1. Eddies and conversion of NADW to AAIW*

To better understand how eddies affect dense-water transformation near the Antarctic divergence, we consider the vertical density structure south of the PF. Because of the presence of many closed contours of barotropic streamfunction associated with the Ross and Weddell gyres, averaging along streamlines is not easy to interpret south of 60°S. Therefore, we simply compare here the zonally averaged section of potential density in the eddying and the non-eddying models (Fig. 2). Near the surface and south of 60°S, the eddying model's upper circumpolar deep water (UCDW, $\sigma_\theta = 27.4{-}27.6$) layer is thicker, which corresponds to a weakening of meridional and vertical density gradients in the upper ocean. Because the near-surface circulation in this region is dominated by the vertical Ekman pumping, this weakening leads to a decrease in the density of upwelled water. Being lighter, the upwelled water masses undergo less diapycnal transformation near the ocean surface. The eddy-induced reduction of the diapycnal transformation of dense water near the Antarctic divergence has been demonstrated in previous theoretical studies (Hallberg and Gnanadesikan, 2001; Karsten and Marshall, 2002). In the non-eddying simulation, the total diapycnal transport across the $\sigma_0 = 27.5$ integrated from 64°S to 58°S is 26 Sv, whereas in the eddying simulation it is only 13 Sv. Thus, the eddy-induced thickening of UCDW in the upper ocean near the Antarctic divergence leads to a reduction in the transformation of dense NADW-LCDW ($\sigma_\theta = 27.6{-}28.0$) to lighter AAIW/SAMW in the eddying model.

The eddy-induced increase of UCDW thickness in the upper thermocline south of 58°S is roughly compensated by a decrease in thickness at intermediate depths between 45°S and 58°S (Fig. 8). Thus eddies redistribute water within the UCDW layer, smoothing out meridional differences in its thickness across the ACC. In the eddying simulation, there is also a 24% decrease in volume of AAIW at 45°S and a 17% increase of NADW volume at 50°S. Thus, it appears that less NADW is converted into AAIW in the Southern Ocean. Determining the actual rate of this transformation is one key to improving understanding of the thermohaline circulation and climate in general. For example, Saenko et al. (2003) found two stable modes of the thermohaline circulation that depend on the relative difference between densities of NADW and AAIW, which is

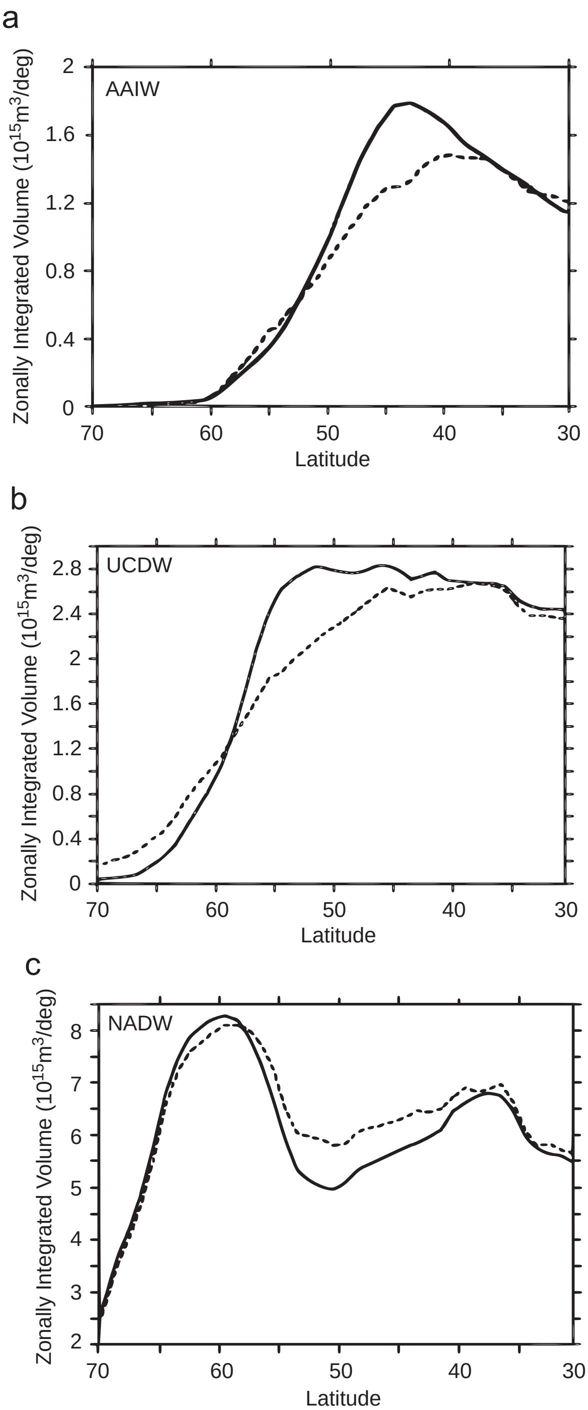


**Fig. 8.** Zonally integrated volumes of AAIW (top), UCDW (middle) and NADW (bottom) for the non-eddying model (solid line) and the eddying model (dashed line) south of 30°S.

in turn connected to the rate at which NADW is transformed into AAIW.

The formation of AAIW is thought to result essentially from some combination of two processes: (i) the isopycnal subduction of fresh AASW along the Antarctic polar frontal zone (APFZ) and (ii) the convection-driven vertical mixing during winter within the freshest and coldest variety of SAMW north of the SAF (Tomczak, 1999). Both mechanisms involve downward transport of freshwater. Rapid ventilation of intermediate water is tightly linked to the capacity of surface freshwater to sink, which depends in turn on the vertical buoyancy profile. Thus, to gain insight into why eddies lead to reduced and more localized AAIW ventilation, we studied how eddies affect the buoyancy fluxes in the Southern Ocean, which alters vertical and meridional freshwater transport.

### 4.2. AAIW ventilation and eddy fluxes

As an indicator of the contribution of eddies to meridional buoyancy transport, we computed the time-mean meridional eddy flux of buoyancy at each grid point using the identity

$$\overline{v'b'} = \overline{vb} - \overline{v}\overline{b} \tag{2}$$

where $v$ is the meridional component of velocity and $b$ is local buoyancy. Following the Reynolds convention, the overbar represents the annual mean and the prime is deviation from the annual mean. Temporal deviations were computed from 5-day snapshots. We found these eddy fluxes to be negligible over the whole southern extratropics in the coarse-resolution version of the model. Thus, we show only the results from the eddying simulation. We further split the buoyancy transport term into two parts: one part due to eddy heat transport and the other part due to eddy freshwater transport. Fig. 9 shows the zonal integrals of these two quantities calculated for both the World Ocean and the individual ocean basins south of 40°S. Eddies transport buoyancy poleward over a large part of southern high and mid-latitudes. Heat transport dominates the buoyancy transport over most of the Southern Ocean, except north of 45°S where freshwater transport becomes important. North of 55°S, most of the buoyancy transport due to eddy heat transport and eddy freshwater transport occurs in the Indian sector of the Southern Ocean. Much less but still a substantial contribution of the eddy buoyancy transport occurs in the Atlantic Ocean north of 45°S. In the Pacific Ocean, eddies drive an important poleward transport of heat south of 55°S. Yet, eddy fluxes of buoyancy are negligible in the Pacific sector's 55°S–40°S latitudinal band where AAIW subducts and reaches intermediate depths. This explains the Pacific sector's small reduction of AAIW ventilation when moving from the non-eddying to the eddying resolution.

Further study of the vertical structure of the eddy heat transport, which dominates the buoyancy transport in the Southern Ocean, reveals that it is largest in the upper 1000 m, with peak transport at 500 m (Fig. 10). Thus eddy activity tends to warm these upper-ocean waters north of

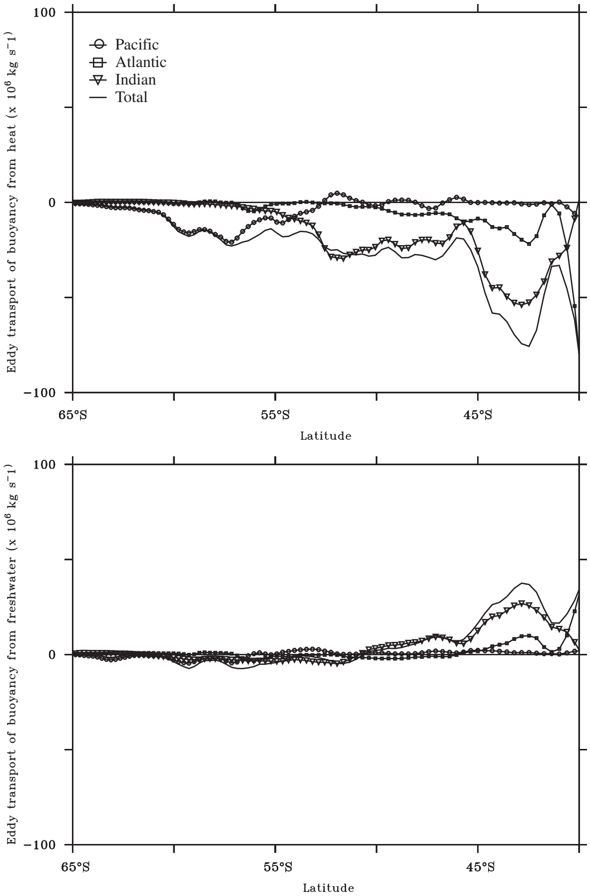


**Fig. 9.** The eddying model's meridional eddy transport of buoyancy ($10^6\,kg\,s^{-1}$) due to (top) heat and (bottom) freshwater over the World Ocean and in the different individual basins.

the SAF. That warming increases the vertical stratification particularly important at intermediate depths (around 500 m), thereby limiting the sink of freshwater further below. This eddy-induced warming and the associated reduction in the freshwater penetration is particularly apparent in streamwise averages of simulated temperature and salinity over the upper 1000 m (Fig. 11). The increased stratification also limits the deep wintertime convection in the southern mid latitudes as shown in Fig. 12. Relative to the non-eddying models, the simulated mixed layer is generally shallowest in regions of deep convection in the eddying model, particularly in the southeastern Indian Ocean. The winter mixed layer in both the non-eddying simulations are too deep compared to observations (de Boyer Montégut et al., 2004), whereas it is generally more realistic in the eddying model. Thus explicitly resolving mesoscale eddies reduces the transformation of cold and fresh SAMW into AAIW through convective mixing.

In summary, in our simulations, explicitly resolving eddies increases the volume of the UCDW near the Antarctic divergence and reduces the upwelling of dense LCDW/NADW, thereby reducing its conversion into light AAIW at ocean surface. North of the SAF, eddies act to

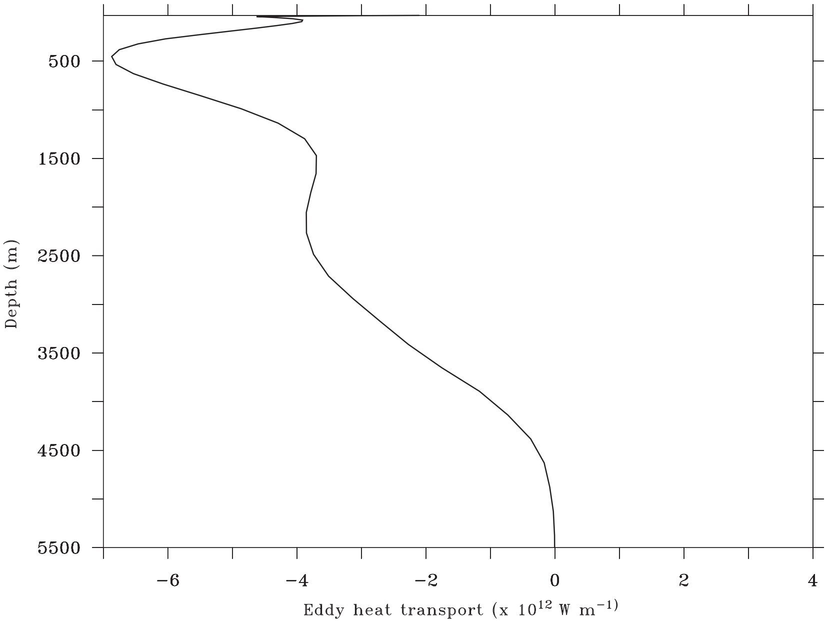


**Fig. 10.** The eddying model's vertical profile of the meridional eddy heat transport ($W\,m^{-1}$) averaged between 55°S and 40°S.

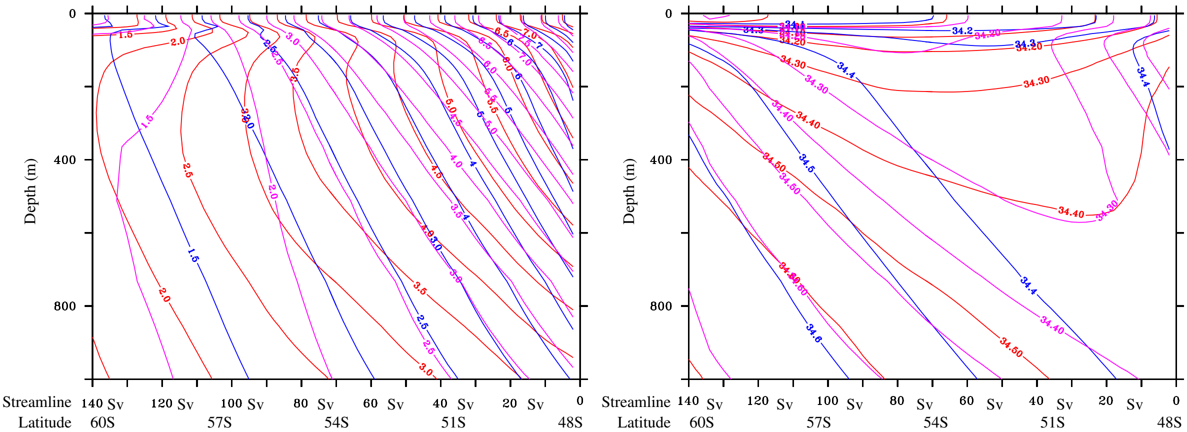


**Fig. 11.** Temperature (left) and salt (right) averaged along bartropic streamlines in the upper 1000 m, as simulated by the non-eddying model (blue), the eddying model (red) and the non-eddying model with GM (purple). The northernmost and southernmost bounds of the barotropic transport that go through the Drake Passage are 0 and 140 Sv respectively. (For interpretation of the references to color in this figure legend, the reader is referred to the web version of this article.)

warm the upper ocean thereby amplifying vertical stratification at intermediate depths. This increased vertical stratification reduces the subduction of freshwater and limits deep wintertime convection, both of which reduce intermediate water ventilation. Fig. 13 summarizes the fundamental differences between the eddying and the non-eddying models.

Higher eddy activity in the Indian sector relative to the Pacific sector has no single explanation. Regional differences in atmospheric forcing and bottom topography probably both contribute. The Indian sector's much stronger wind stress injects more energy into the flow (Fig. 14). This greater energy input may partly explain the Indian sector's stronger eddy energy. The complicated link between the wind energy and the eddy activity in the Southern Ocean has been illustrated in previous studies (Hallberg and Gnanadesikan, 2006; Meredith and Hogg, 2006; Hogg et al., 2008). Bottom topography may also play an important role in the Indian sector because it is steeper and more uneven than the nearly flat-bottomed southeast Pacific. These non-uniform eddy fluxes along the ACC likewise imply a patchy distribution of AAIW source regions. The patchy distribution of AAIW formation in our eddying model contrasts with results from some previous studies where the effects of eddies have been parameterized in coarse-resolution models (Marsh et al., 2000; Sorensen et al., 2001). In those studies, AAIW also formed nearly homogeneously along the SAF. Our work

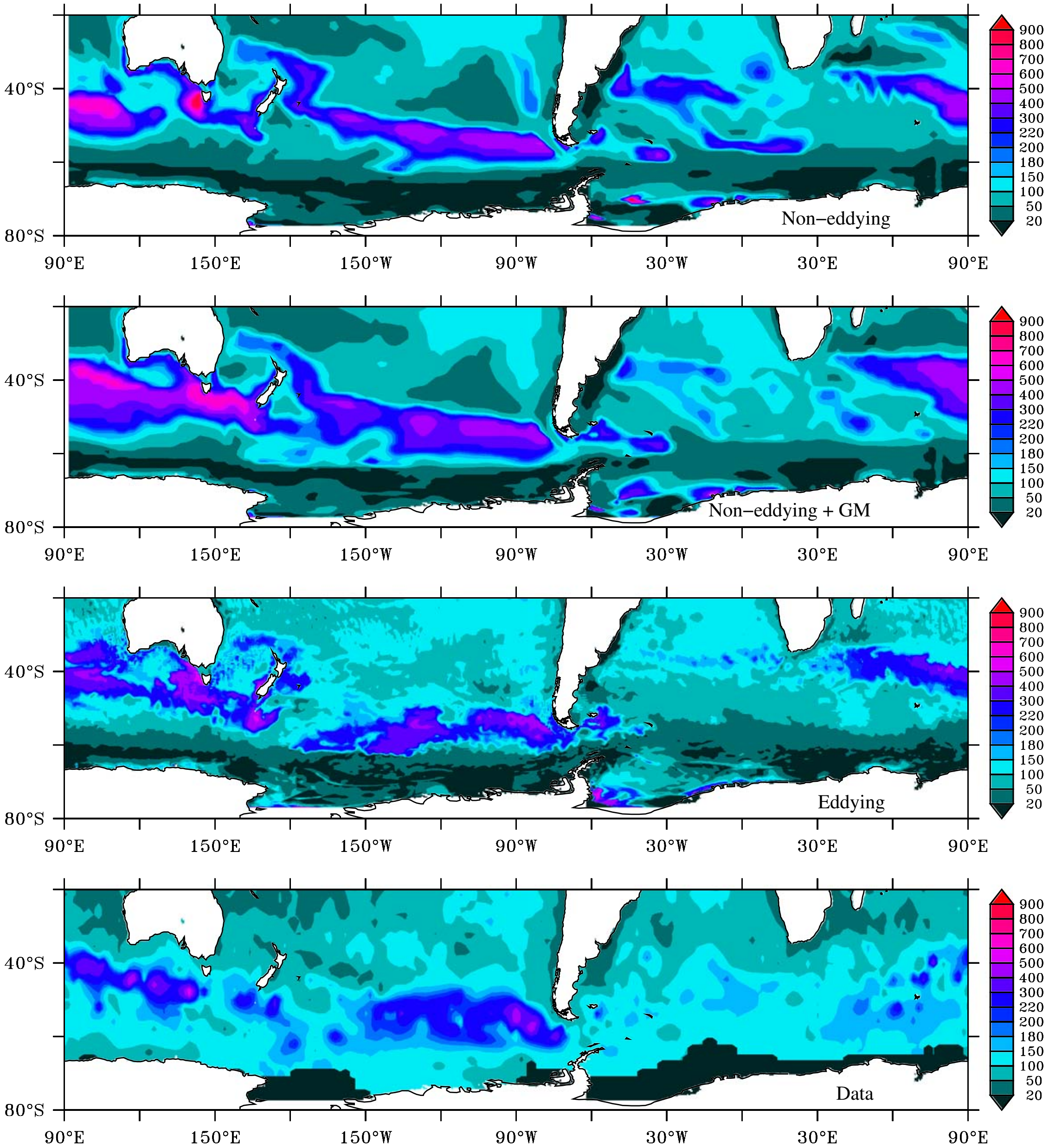


**Fig. 12.** Wintertime mixed layer depth (m) in the Southern Hemisphere (September), as (from top to bottom) simulated in the non-eddying model, the non-eddying model with the GM parameterization, the eddying simulation, and from data (climatology of de Boyer Montégut et al., 2004).

suggests that this is a misrepresentation of the effects of eddies on AAIW formation, which derives in part from an inadequate eddy parameterization.

### *4.3. The poor performance of GM in the Indian sector*

To better understand inadequacies of GM parameterization, we compare the eddy transfer coefficient computed from Eq. (1) between the eddying and non-eddying resolutions. This coefficient represents the potential of the simulated circulation to adiabatically generate eddy advective fluxes from the mean flow. In the eastern portion of Indian Ocean, the GM eddy transfer coefficient is much weaker at the non-eddying resolution (Fig. 15). This coefficient also increases during summer in the Indian Ocean as the mixed layer shoals. The poor performance of the GM parameterization in the Indian Ocean at the non-eddying resolution appears to be directly linked to its exaggerated wintertime mixed layer depth (Fig. 12). A deep mixed layer has a reduced mean vertical stratification, implying a GM eddy transfer coefficient that is too low. In reality, eddy fluxes do not vanish within the mixed layer; rather, they become horizontal allowing transport across density surfaces. These horizontal eddy fluxes help the mixed layer to

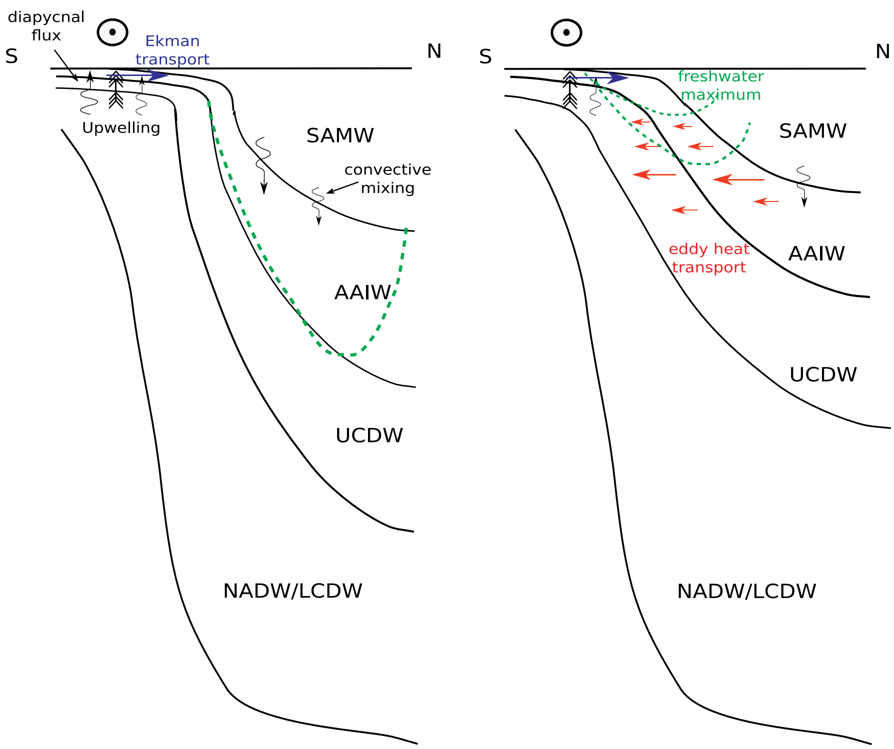


**Fig. 13.** A sketch showing the simulated density structure and the different water masses in the Southern Ocean. For the non-eddying simulation (left), the UCDW layer is too thin around the Antarctic divergence and the dense NADW/LCDW water masses are too shallow. After being upwelled to surface, these water masses are converted into lighter AAIW through strong diapycnal fluxes. AAIW subducts too far to the north, where vertical penetration of AAIW is too deep because stratification is too weak. This weak stratification also promotes excessive deep convective mixing and transformation of dense SAMW into AAIW indicated by the curly arrows. For the eddying simulation (right), the UCDW layer is thicker and displaces denser NADW/LCDW downward. Upwelled waters are not as dense, meaning that diapycnal fluxes near the surface are smaller. Eddy heat transport (red arrows) increases stratification at intermediate depths, thereby limiting the vertical penetration of freshwater and reducing the convective mixing. (For interpretation of the references to color in this figure legend, the reader is referred to the web version of this article.)

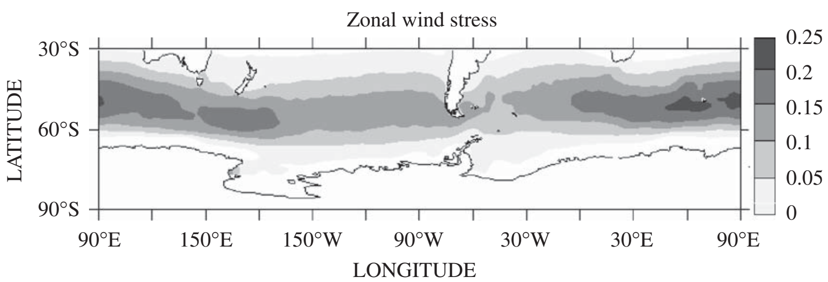


**Fig. 14.** Annual mean zonal wind stress forcing over the Southern Ocean ($N\,m^{-2}$).

restratify and thus to shoal (Boccaletti et al., 2007). The GM parameterization fails to represent the effects of mesoscale eddies in the upper ocean because it represents an adiabatic formulation of baroclinic eddies, whereas near-surface ocean circulation and eddy fluxes are largely horizontal and diabatic (Ferrari et al., 2008; Ferreira and Marshall, 2006; Boccaletti et al., 2007). However, in order to maintain numerical stability in the non-eddying simulation, the slopes of isopycnal surfaces are bounded by $\frac{1}{100}$ everywhere. This introduces some diabatic fluxes in regions with steep isopycnal surfaces and particularly around deep convection sites (Gerdes et al., 1991; Danabasoglu and McWilliams, 1995). Yet, these fluxes are driven by pure numerical stability constraints and do not rely on any satisfactory theoretical framework to describe vertical profiles of the eddy fluxes in the mixed layer. Our comparison reveals that the role played by mesoscale eddies in the mixed layer is not properly accounted for by the GM parameterization, but is crucial and their representation should be improved. The failure of the GM parameterization in the Indian basin introduces erroneous exchange between the mixed layer and interior ocean, which further affects air-sea tracer fluxes. Consequently, one would expect that patterns of AAIW

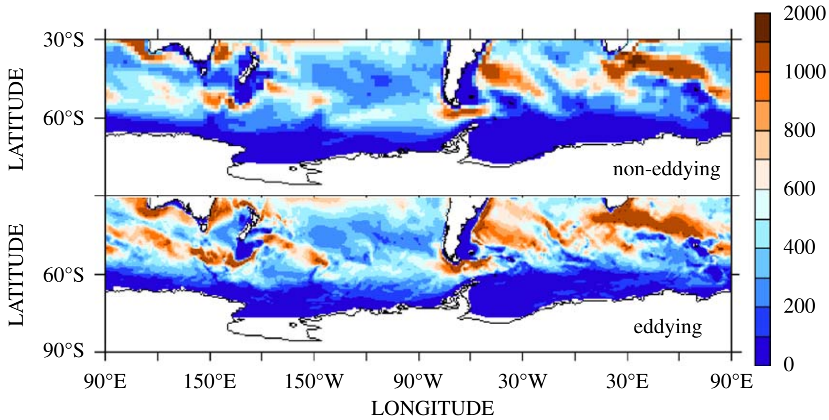


**Fig. 15.** The annual mean GM eddy transfer coefficient ($m^2\,s^{-1}$) computed from Eq. (1) for the non-eddying model grid (top) and the eddying model grid (bottom).

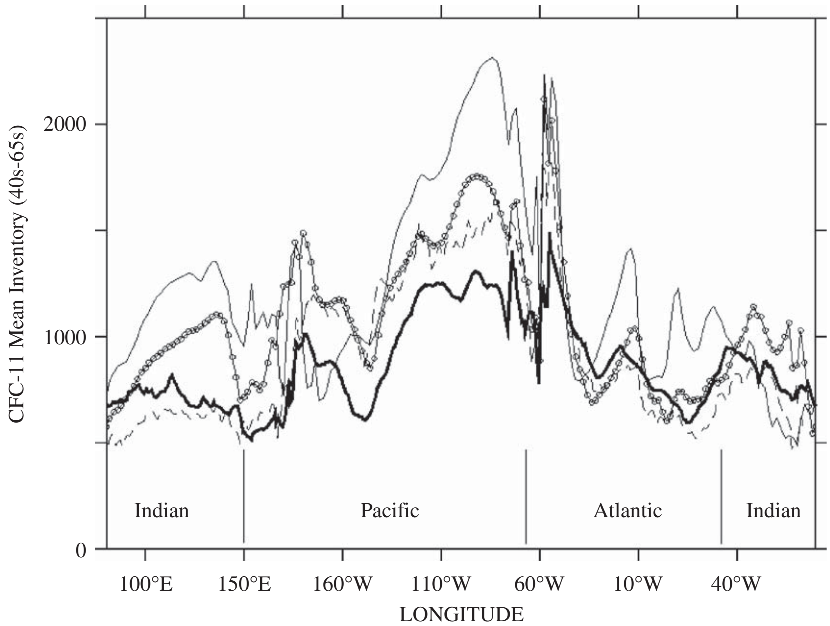


**Fig. 16.** CFC-11 inventory in the AAIW layer at end of 1994 averaged meridionally between 65°S and 40°S (pmol $m^{-2}$), from the GLODAP data (thick solid line) and as simulated in the non-eddying model (thin solid line), the non-eddying model with GM parameterization (line with small circles), and the eddying simulation (thin dashed line).

formation would also differ between these two models. Model-data comparison of the meridionally averaged CFC-11 inventory between 65°S and 40°S (Fig. 16) indicates that AAIW ventilation in the Indian Ocean of the non-eddying model, with or without GM, is much too strong, whereas that in the eddying model is only slightly underestimated. Thus the non-eddying model with GM offers less contrast between basins than does the eddying model.

In summary, the GM parameterization is known to improve the vertical density structure in the ocean interior, but it should be adapted to properly account for diabatic eddy-induced transport in the mixed layer. Ferrari et al. (2008) have initiated a recent research effort in this direction. Their new parameterization is meant to offer a more realistic representation of the effect of eddies near the surface boundary as well as in the ocean interior. Future work should test how this new parameterization may improve simulated AAIW ventilation and subduction.

### 4.4. Comparison with previous work

Two previous coarse-resolution model studies (England et al., 1993; Saenko and England, 2003) are somewhat consistent with the McCartney (1977) picture of AAIW formation. However, it is not immediately apparent why these model studies succeed more than others in producing the non-uniform distribution of AAIW formation. For instance, these models differ from our eddying simulation not only in their coarser, non-eddying resolution, but also in their forcing and model physics. Using a non-eddying model with an isopycnal lateral diffusion scheme but without GM, England et al. (1993) simulated enhanced AAIW formation in the southeast Pacific that was dominated by vertical convection. However, that model configuration exhibited too much AAIW formation owing to excess freshwater originating from isopycnal mixing in the polar frontal zone of the South Indian Ocean, particularly south of Australia as reported by England (1993) (see his Fig. 15b).

More recently, Saenko and England (2003) used a coupled atmosphere-ocean climate model with the GM parameterization. With a passive age tracer, they identified rapid ventilation of intermediate water around the southern tip of South America, consistent with our eddying model results. However, they also found an additional zone of rapid ventilation in the southeast Indian Ocean (see their Fig. 6). The contrast found between the Indian and the Pacific sectors in their study is much less than that found in our eddying model, which is supported by our model-data comparison of the CFC-11 inventory. Our main contribution to this debate is to show that one can move from simulating the nearly uniform distribution to simulating a more realistic heterogeneous distribution simply by increasing horizontal model resolution.

## 5. Summary and conclusions

The formation and ventilation of AAIW is a matter of ongoing debate opposing one view where there is nearly uniform circumpolar formation, as proposed by Sverdrup et al. (1942), with another view where there is a more localized distribution, as proposed by McCartney (1977). In an attempt to shed light on this debate, we have investigated the role of the mesoscale eddies by making simulations in the coupled ocean-ice model ORCA-LIM at eddying and non-eddying resolutions (neither with GM). Overall, the total volume of AAIW at 45°S was 24% less in the eddying simulation, which corresponded to a thinning of the AAIW layer by 32% in the Indian sector and 11% in the Pacific sector. Simulated CFC-11 distributions within the AAIW layer reveal that intermediate water ventilation and subduction have a near-uniform, circumpolar distribution in the non-eddying simulation, but a non-uniform distribution concentrated in the southeastern Pacific and in the westernmost South Atlantic in the eddying simulation. The increase in horizontal resolution also yields better agreement with CFC-11 observations.

Eddy-induced isopycnal mixing, particularly important in the UCDW layer, reduces the diapycnal flux that converts dense upwelled NADW into less dense AAIW near the Antarctic divergence. Further north to the SAF, poleward eddy heat transport increases ocean stratification at intermediate depths, thereby limiting the vertical penetration of AAIW and reducing the wintertime deep convective mixing at the base of the SAMW.

We hypothesize that the relatively high eddy activity in the southeastern portion of the Indian basin results primarily from the strong wind stress characterizing this region. As a consequence, when moving from the non-eddying to the eddying model, the sink of freshwater in the AAIW subduction zone is reduced by an eddy-induced warming at intermediate depths that is much larger in the Indian sector than in the Pacific sector. This also results in greater inhibition of the wintertime convection in the southern mid-latitudes higher in the southeast Indian Ocean than in the South Pacific Ocean. Therefore, the main reason why the AAIW is not formed uniformly along the ACC in the eddying model is due to the heterogeneity of the eddy fluxes along the ACC and ultimately the external factors that generate them.

We have compared results from the eddying version of the model to those from a version of the non-eddying model that includes the GM parameterization. Because this parameterization is fundamentally adiabatic, it does not properly account for the diabatic horizontal eddy fluxes in the mixed layer. As a result, the non-eddying model with the GM parameterization overestimates the rate of AAIW ventilation, particularly in the Indian Ocean where the mixed layer is much too deep during the winter, which leads to a more uniform circumpolar distribution of AAIW subduction around the ACC than found in the eddying model. This finding may partly explain why most previous studies with coarse-resolution GCMs that include the GM parameterization support the original Sverdrup et al. (1942) paradigm of uniform AAIW formation. Partial exceptions include non-eddying modeling studies by England et al. (1993) and Saenko and England (2003) who did find enhanced AAIW formation in the southeast Pacific, but who also found substantial AAIW formation in the Indian Ocean. Results from our eddying model, which exhibits greater contrast in AAIW formation between the Indian and the Pacific sectors, suggest that coarse-resolution models may tend to overestimate the ventilation of AAIW in the Indian sector of the southern extratropics; hence, they may also overestimate associated uptake of anthropogenic $CO_2$ and heat. Further simulations at higher resolutions are required to determine the extent to which further increases in horizontal resolution may alter these findings. This study suggests that there is a need for ocean models to adopt higher resolution or incorporate improved parameterizations that properly represent the effects of eddies not only in the ocean interior but also in the deep mixed layers.

## Acknowledgments

We thank C. Levy, C. Talendier, C. Ethé, R. Benshila, S. Masson, and other contributors to the ESOPA group at LOCEAN for the general support, improvements, and maintenance of the ocean model OPA-ORCA. We also thank B. Barnier, A.-M. Treguier, J.-M. Molines, G. Madec, and other members of the DRAKKAR project for discussions, particularly their expertise concerning the model configurations used here. Support for this research has come from the French Commissariat à l'Energie Atomique (CEA), the EU CARBOOCEAN Project (Contract no. 511176

[GOCE]) and the Swiss Federal Institute of Technology Zurich (ETH Zurich). Computations were performed at CEA (CCRT) supercomputing center. The IAEA is grateful for the support provided to its Marine Environmental Laboratory by the Government of the Principality of Monaco.

## References


Berliand, M.E., Strokina, T., 1980. Global Distribution of the Total Amount of Clouds. Hydrometeorological Publishing House, Leningrad, Russia, 71pp. (in Russian).

Blanke, B., Delecluse, P., 1993. Low frequency variability of the tropical Atlantic Ocean simulated by a general circulation model with two different mixed layer physics. J. Phys. Oceanogr. 23, 1363–1388.

Boccaletti, G., Ferrari, R., Fox-Kemper, B., 2007. Mixed layer instabilities and restratification. J. Phys. Oceanogr. 37, 2228–2250.

Cox, M., 1987. Isopycnal diffusion in a z-coordinate ocean model. Ocean Modelling 74, 1–9.

Danabasoglu, G., McWilliams, J.C., Gent, P.R., 1994. The role of mesoscale tracer transports in the global ocean circulation. Science 264, 1123–1126.

Danabasoglu, G., McWilliams, J.C., 1995. Sensitivity of the global ocean circulation to parameterizations of mesoscale tracer transports. J. Climate 8, 2967–2987.

de Boyer Montégut, C., Madec, G., Fischer, A.S., Lazar, A., Iudicone, D., 2004. Mixed layer depth over the global ocean: an examination of profile data and a profile-based climatology. J. Geophys. Res. 109, C12003.

Dixon, K.W., Bullister, J.L., Gammon, R.H., Stouffer, R.J., 1996. Examining a coupled climate model using CFC-11 as an ocean tracer. Geophys. Res. Lett. 23 (15), 1957–1960.

Doney, S., Bullister, J., 1992. A chlorofluorocarbon section in the eastern North Atlantic. Deep-Sea Res. 39, 1857–1883.

Doney, S.C., Bullister, J.L., Wanninkhof, R., 1998. Climatic variability in upper ocean ventilation rates diagnosed using chlorofluorocarbons. Geophys. Res. Lett. 25, 1399–1402.

Duffy, P.B., Caldeira, K., Selvaggi, J., Hoffert, M.I., 1997. Effects of subgrid-scale mixing parameterizations on simulated distribution of natural $^{14}$C, temperature, and salinity in a three-dimensional ocean general circulation model. J. Phys. Oceanogr. 27, 498–523.

Dutay, J.-C., Bullister, J., Doney, S.C., Orr, J.C., Najjar, R.G., Caldeira, K., Campin, J.-M., Drange, H., Follows, M., Gao, Y., Gruber, N., Hecht, M.W., Ishida, A., Joos, F., Lindsay, K., Madec, G., Maier-Reimer, E., Marshall, J.C., Matear, R., Monfray, P., Mouchet, A., Plattner, G.K., Sarmiento, J.L., Schlitzer, R., Slater, R.D., Totterdell, I.J., Weirig, M.-F., Yamanaka, Y., Yool, A., 2002. Evaluation of ocean model ventilation with CFC-11: comparison of 13 global ocean models. Ocean Modelling 4, 89–120.

England, M.H., 1993. Representing the global-scale water masses in ocean general circulation models. J. Phys. Oceanogr. 22, 1523–1552.

England, M.H., 1995. Using chlorofluorocarbons to assess ocean climate models. Geophys. Res. Lett. 22, 3051–3054.

England, M.H., Godfrey, J.S., Hirst, A.C., Tomczak, M., 1993. The mechanism for Antarctic intermediate water renewal in a World Ocean model. J. Phys. Oceanogr. 23, 1553–1560.

England, M.H., Hirst, A.C., 1997. Chlorofluorocarbon uptake in a World Ocean model 2. Sensitivity to surface thermohaline forcing and subsurface mixing parameterization. J. Geophys. Res. 102, 15709–15731.

Ferrari, R., McWilliams, J.C., Canuto, V., Dubovikov, D., 2008. Parameterization of eddy fluxes at the ocean boundaries. J. Climate 21, 2770–2787.

Ferreira, D., Marshall, J., 2006. Formulation and implementation of a residual-mean ocean circulation model. Ocean Modelling 13, 86–107.

Fichefet, T., Maqueda, M.M., 1997. Sensitivity of a global sea ice model to the treatment of ice thermodynamics and dynamics. J. Geophys. Res. 102, 12609–12646.

Fine, R., 1993. Circulation of Antarctic intermediate water in the Indian Ocean. Deep-Sea Res. I 40, 2021–2042.

Fine, R., Maillet, K., Sullivan, K., Willey, D., 2001. Circulation and ventilation flux of the Pacific Ocean. J. Geophys. Res. 106, 22159–22178.

Gammon, R.H., Cline, J., Wisegarver, D., 1982. Chlorofluoromethanes in the northeast Pacific Ocean: measured vertical distributions and application as transient tracer of upper ocean mixing. J. Geophys. Res. 87, 9441–9454.

Gaspar, P., Gregorius, Y., Lefevre, J.M., 1990. A simple eddy kinetic energy model for simulation of oceanic vertical mixing tests at Station Papa and Long-Term Upper Ocean Study Site. J. Geophys. Res. 95, 16179–16193.

Gent, P.R., Bryan, F.O., Danabasoglu, G., Doney, S.C., Holland, W.R., Large, W.G., McWilliams, J.C., 1998. The NCAR climate system model global ocean component. J. Climate 11, 1287–1306.

Gent, P.R., McWilliams, J.C., 1990. Isopycnal mixing in ocean circulation models. J. Phys. Oceanogr. 20, 150–155.

Gent, P.R., Willebrand, J., McDougall, T.J., McWilliams, J.C., 1995. Parameterizing eddy-induced tracer transports in ocean circulation models. J. Phys. Oceanogr. 25, 463–474.

Gerdes, R., Koberle, C., Willebrand, J., 1991. The influence of numerical advection schemes on the results of ocean general circulation models. J. Climate Dyn. 5, 211–226.

Gille, J.C., Lyjak, L.V., Smith, A.K., 1987. The global residual mean circulation in the middle atmosphere for northern winter period. J. Atmos. Sci. 44, 1437–1452.

Goose, H., 1997. Modeling the large scale behaviour of the coupled ocean-sea ice system. Ph.D. Thesis, Université Catholique de Louvain, Louvain-la-Neuve, Belgium.

Hallberg, R., Gnanadesikan, A., 2006. The role of eddies in determining the structure and response of the wind-driven Southern Hemisphere overturning: results from the modeling eddies in the Southern Ocean project. J. Phys. Oceanogr. 36, 2232–2252.

Hallberg, R.W., Gnanadesikan, A., 2001. An exploration of the role of transient eddies in determining the transport of a zonally reentrant current. J. Phys. Oceanogr. 31, 3312–3330.

Hirst, A., McDougall, T.J., 1996. Deep-water properties and surface buoyancy flux as simulated by a z-coordinate model including eddy-induced advection. J. Phys. Oceanogr. 26, 1320–1343.

Hirst, A.C., Cai, W., 1994. Sensitivity of a World Ocean GCM to changes in subsurface mixing parameterization. J. Phys. Oceanogr. 24, 1256–1280.

Hogg, A.M., Meredith, M.P., Blundell, J.R., Wilson, C., 2008. Eddy heat flux in the Southern Ocean: response to variable wind forcing. J. Climate 21, 608–620.

Ivchenko, V., Richards, K., Stevens, D., 1996. The dynamics of the Antarctic circumpolar current. J. Phys. Oceanogr. 26, 753–774.

Jakobsson, M., Cherkis, N., Woodward, J., Coakley, B., Macnab, R., 2000. A new grid of Arctic bathymetry: a significant resource for scientists and mapmakers. Eos Trans AGU 81(9), p. 89, 93, 96.

Kalnay, E., Kanamitsu, M., Kistler, R., Collins, W., Deaven, D., Gandin, L., Iredell, M., Saha, S., White, G., Woollen, J., Zhu, Y., Chelliah, M., Ebisuzaki, W., Higgins, W., Janowiak, J., Mo, K.C., Ropelewski, C., Wang, J., Leetma, A., Reynolds, R., Jenne, R., Joseph, D., 1996. The NCEP/NCAR 40-year reanalysis project. Bull. Am. Meteor. Soc. 77, 437–471.

Karsten, R.H., Marshall, J., 2002. Constructing the residual circulation of the ACC from observations. J. Phys. Oceanogr. 32, 3315–3327.

Key, R.M., Lee, C.L.S.K., Wanninkhof, R., Bullister, J., Feely, R.A., Millero, F.J., Mordy, C., Peng, T.-H., 2004. A global ocean carbon climatology: results from Global Data Analysis Project (GLODAP. Global Biogeochem. Cycles 18, GB4031.

Lachkar, Z., Orr, J.C., Dutay, J.C., Delecluse, P., 2007. Effects of mesoscale eddies on global ocean distributions of CFC-11, $CO_2$ and $\delta^{14}$C. Ocean Sci. 3, 461–482.

Large, W.G., Danabasoglu, G., Doney, S.C., McWilliams, J.C., 1997. A review and a model with a non-local boundary layer parameterization. Rev. Geophys. 32, 363–403.

Lee, M.M., Marshall, D.P., Williams, R.G., 1997. On the eddy transfer of tracers: advective or diffusive. J. Mar. Res. 55, 483–505.

Lee, M.M., Coward, A., 2003. Eddy mass transport for the Southern Ocean in an eddy-permitting global ocean model. Ocean Modelling 3, 249–266.

Levitus, S., Boyer, T., Conkright, M., O'Brian, T., Antonov, J., Stephens, C., Stathopolos, L., Johnson, D., Gelfeld, R., World Ocean Database 1998. Technical Report, NOAA Atlas NESDID18, 1998.

Lythe, M., Vaughan, D., 2001. BEDMAP: a new ice thickness and subglacial topograpic model of Antarctica. J. Geophys. Res. 106, 11335–11351.

Madec, G., Delecluse, P., Imbard, M., Lévy, C., 1998. OPA version 8.0, Ocean General Circulation Model, Reference Manual. Note of the IPSL Modelling Pole 11, IPSL.

Madec, G., Imbard, M., 1996. A global ocean mesh to overcome the North Pole singularity. Climate Dyn. 12, 381–388.

Marsh, R., Nurser, A.J., Megann, A., New, A., 2000. Water mass transformation in the Southern Ocean of a global isopycnal coordinate GCM. J. Phys. Oceanogr. 30, 1013–1045.
Marshall, D., 1997. Subduction of water masses in an eddying ocean. J. Mar. Res. 55, 201–222.
Marshall, J., Jones, H., Karsten, R., Wardle, R., 2002. Can eddies set ocean stratification? J. Phys. Oceanogr. 32, 26–38.
Marshall, J., Olbers, D., Ross, H., Wolf-Gladrow, D., 1993. Potential vorticity constraints on the dynamics and hydrography of the Southern Ocean. J. Phys. Oceanogr. 23, 465–487.
Marshall, J., Radko, T., 2003. Residual-mean solutions for the Antarctic circumpolar current and its associated overturning circulation. J. Phys. Oceanogr. 33, 2341–2354.
McCartney, M.S., 1977. Subantarctic mode water. A Voyage of Discovery. Pergamon, New York, pp. 103–119.
McCartney, M.S., 1982. The subtropical recirculation of mode waters. J. Mar. Res. 40 (Suppl.), 427–464.
Meredith, M.P., Hogg, A.M., 2006. Circumpolar response of Southern Ocean eddy activity to a change in the Southern Annular Mode. Geophys. Res. Lett. 33, L16608.
Molinelli, E.J., 1981. The Antarctic influence on Antarctic intermediate water. J. Mar. Res. 39, 267–293.
Orr, J.C., Monfray, P., Maier-Reimer, E., Mikolajewicz, U., Palmer, J., Taylor, N.K., Toggweiler, J.R., Sarmiento, J.L., Quéré, C.L., Gruber, N., Sabine, C.L., Key, R.M., Boutin, J., 2001. Estimates of anthropogenic carbon uptake from four three-dimensional global ocean models. Global Biogeochem. Cycles 15, 43–60.
Pedlosky, J., 1987. Geophysical Fluid Dynamics. Springer, New York, 710pp.
Piola, A., Georgi, D., 1982. Circumpolar properties of Antarctic intermediate water and subantarctic mode water. Deep-Sea Res. 29, 687–711.
Price, J.F., 2001. Subduction, 357–371. In: Siedler, G., Church, J., Gould, J. (Eds.), Ocean Circulation and Climate: Observing and Modelling the Global Ocean. Academic Press, London, p. 715.
Ribbe, J., 1999. On wind-driven mid-latitude convection in ocean general circulation models. Tellus 51A, 517–525.
Rintoul, S.R., Hughes, C.W., Olbers, D., 2001. The Antarctic circumpolar system. Ocean Circulation and Climate. Academic, London, pp. 271–302.
Sabine, C.L., Feely, R.A., 2001. Comparison of recent Indian Ocean anthropogenic $CO_2$ with a historical approach. Global Biogeochem. Cycles 15, 31–42.
Sabine, C.L., Feely, R.A., Gruber, N., Key, R.M., Lee, K., Bullister, J.L., Wanninkhof, R., Wong, C.S., Wallace, D.W.R., Tilbrook, B., Millero, F.J., Peng, T.-H., Kozyr, A., Ono, T., Rios, A., 2004. The ocean sink for anthropogenic $CO_2$. Science 305, 367–370.
Sabine, C.L., Feely, R.A., Key, R.M., Bullister, J.L., Millero, F.J., Lee, K., Peng, T.-H., Tilbrook, B., Ono, T., Wong, C.S., 2002. Distribution of anthropogenic $CO_2$ in the Pacific Ocean. Global Biogeochem. Cycles 16, 1083.
Saenko, O.A., England, M.H., 2003. A region of enhanced northward Antarctic intermediate water transport in a coupled climate model. J. Phys. Oceanogr. 33, 1528–1535.
Saenko, O.A., Weaver, A.J., Gregory, J.M., 2003. On the link between the two modes of the ocean thermohaline circulation and the formation of global-scale water masses. J. Climate 16 (17), 2797–2801.
Santoso, A., England, M.H., 2004. Antarctic intermediate water circulation and variability in a coupled climate model. J. Phys. Oceanogr. 34, 2160–2179.
Sarmiento, J.L., Le Quéré, C., 1996. Oceanic carbon dioxide uptake in a model of century-scale global warming. Science 274, 1346–1350.
Sasai, Y., Ishida, A., Yamanaka, Y., Sasaki, H., 2004. Chlorofluorocarbons in a global ocean eddy-resolving OGCM: pathway and formation of Antarctic bottom water. Geophys. Res. Lett. 31, L12305.
Schmitz, W.J., 1996. On the World Ocean circulation. The Pacific and Indian Oceans—A Global Update, vol. ii. Technical Report, Woods Hole Oceanogr. Inst., WHOI-96-08, 241pp.
Sen Gupta, A., England, M., 2004. Evaluation of interior circulation in a high resolution global ocean model, part i: deep and bottom waters. J. Phys. Oceanogr. 34, 2592–2614.
Smith, W.H.F., Sandwell, D.T., 1997. Global seafloor topography from satellite altimetry and ship depth soundings. Science 277, 1957–1962.
Sorensen, J.V.T., Ribbe, J., Shaffer, G., 2001. Antarctic intermediate water mass formation in ocean general circulation models. J. Phys. Oceanogr. 31, 3295–3311.
Steele, M., Morley, R., Ermold, W., 2001. PHC: a global ocean hydrography with a high quality Arctic Ocean. J. Climate 14, 2079–2087.
Sverdrup, H.U., Johnson, M.W., Fleming, R.H., 1942. The Oceans: Their Physics, Chemistry, and General Biology. Prentice-Hall, Englewood Cliffs, NJ.
Talley, L.D., 1996. Antarctic intermediate water in the South Atlantic. The South Atlantic. Springer, Berlin, pp. 219–238.
Tomczak, M., 1999. Some historical, theoretical and applied aspects of quantitative water mass analysis. J. Mar. Res. 57, 275–303.
Trenberth, K.E., Olson, J.G., Large, W.G., 1989. A global ocean wind stress climatology based on ECMWF analyses, Report NCAR/TN-338 +STR, National Center for Atmos. Res., Boulder, Colorado, 93pp.
Vallis, G.K., 2000, Thermocline theories and WOCE: a mutual challenge. International WOCE Newsletter, 39, WOCE International Project Office, Southampton, United Kingdom, pp. 3–5.
Visbeck, M., Marshall, J., Haine, T., Spall, M., 1997. Specification of eddy transfer coefficients in coarse resolution ocean circulation models. J. Phys. Oceanogr. 27, 381–402.
Wallace, D., Lazier, J., 1988. Anthropogenic chlorofluoromethanes in newly formed Labrador sea water. Nature 332, 61–63.
Xie, P., Arkin, P.A., 1996. Analyses of global monthly precipitation using gauge observations, satellite estimates and numerical model predictions. J. Climate 9, 840–858.